

1 **The application of diffusive gradients in thin films (DGT) for improved understanding of metal**
2 **behaviour at marine disposal sites**

3

4 Ruth Parker¹, Thi Bolam^{1*}, Jon Barry¹, Claire Mason¹, Silke Kröger¹, Lee Warford¹, Briony Silburn¹,
5 Dave Sivyer¹, Silvana Birchenough¹, Andrew Mayes² and Gary R. Fones³

6 ¹ Centre for Environment, Fisheries and Aquaculture Science, Lowestoft Laboratory, Pakefield Road,
7 Lowestoft, Suffolk, UK, NR33 0HT.

8 ²School of Chemistry, University of East Anglia, Norwich Research Park, Norwich, UK, NR4 7TJ

9 ³School of Earth and Environmental Sciences, University of Portsmouth, Burnaby Building, Burnaby
10 Road, Portsmouth, UK, PO1 3QL.

11 * Corresponding author. Tel.: +44 1502 524525; E-mail address: thi.bolam@cefas.co.uk

12

13 **Abstract:**

14 Assessment of the effects of sediment metal contamination on biological assemblages and function
15 remains a key question in marine management, especially in relation to disposal activities. However,
16 the appropriate description of bioavailable metal concentrations within pore-waters has rarely been
17 reported. Here, metal behaviour and availability at contaminated dredged material disposal sites within
18 UK waters were investigated using Diffusive Gradient in Thin films (DGT). Three stations, representing
19 contrasting history and presence of dredge disposal were studied. Depth profiles of five metals were
20 derived using DGT probes as well as discrete analysis of total metal concentrations from sliced cores.
21 The metals analysed were: iron and manganese, both relevant to sediment biogeochemistry; cadmium,
22 nickel and lead, classified as priority pollutants. DGT time-integrated labile flux profiles of the metals
23 display behaviour consistent with increasingly reduced conditions at depth and availability to DGT (iron
24 and manganese), subsurface peaks and a potential sedimentary source to the water column related to
25 the disposal activity (lead and nickel) and release to pore-water linked to decomposition of enriched
26 phytodetritus (cadmium). DGT data has the potential to improve our current understanding of metal
27 behaviour at impacted sites and is suitable as a monitoring tool. DGT data can provide information on
28 metal availability and fluxes within the sediment at high depth-resolution (5 mm steps). Differences
29 observed in the resulting profiles between DGT and conventional total metal analysis illustrates the
30 significance of considering both total metals and a potentially labile fraction. The study outcomes can
31 help to inform and improve future disposal site impact assessment, and could be complemented with
32 techniques such as Sediment Profile Imagery for improved biological relevance, spatial coverage and
33 cost-effective monitoring and sampling of dredge material disposal sites. Additionally, the application
34 of this technology could help improve correlative work on biological impacts under national and
35 international auspices when linking biological effects to more biologically relevant metal
36 concentrations.

37 **Key words:** Dredge material, disposal, metal profiles, sediments, DGT (Diffusive Gradient in Thin-
38 films), labile, bioavailability.

39

40 **1.0 Introduction:**

41 Dredging operations are conducted to remove sediments in order to maintain harbour berths, marinas
42 and channels. The amount of dredging and disposal undertaken worldwide varies depending on a
43 combination of economic, social and legislative needs. This activity is controlled under national and
44 international legislations via licensing authorities, which also have a duty to comply with international
45 conventions on dredging, disposal and marine environmental protection to minimise any adverse
46 environmental consequences (Birchenough et al., 2006; Birchenough et al., 2010).

47 There are 136 sites currently designated for dredged material disposal around the coast of
48 England, mostly in close proximity to the coast and major ports or estuaries. Individual quantities
49 disposed, may range from a few hundred to several million tonnes, with an approximate annual sum of
50 40 million tonnes (Bolam et al., 2010a and 2010b). The nature of the disposed material may vary from
51 soft silts to boulders or even crushed rock according to origin (capital material), although the majority
52 consists of finer material (maintenance dredge material). Disposed material may have differing
53 sediment types, higher loads of organic material and, although regulated, a higher associated loads of
54 various contaminants such as organics or metals, from background or reference sediments. Disposal
55 sites within the UK are selected for annual monitoring based on a tier-based approach that classifies the
56 number of possible issues or environmental concerns that may be associated with dredged material
57 disposal to sea at certain sites (Bolam et al., 2010b). In licensing the disposal of dredged material at
58 sea, several national and international agreements (e.g., the London Protocol of 1996 (LP96), the
59 OSPAR Convention, the Habitats and Species Directive (92/43/EEC), the Wild Birds Directive
60 (79/409/EEC), the Water Framework Directive (2000/60/EC) and the Waste Framework Directive
61 (2008/98/EC)), must be taken into account, to determine whether likely impacts arising from the
62 dredging and disposal are acceptable (MEMG, 2003). Criteria considered under the various
63 conventions and directives include the presence and levels of contaminants in the materials to be
64 disposed of, along with perceived impacts on any sites of conservation value in the vicinity of disposal.

65 A number of different substances are determined as part of the monitoring of disposal sites,
66 such as tributyltin, polycyclic aromatic hydrocarbons, organohalogenes (e.g. PCBs) and metals measured
67 as total metal concentrations in bulk sediments. Additional physico-chemical information, such as
68 sediment particle size, organic carbon and nitrogen content, and sediment profile imagery (SPI), is
69 obtained to further characterise sediment status (Birchenough et al., 2006; Bolam et al., 2010a and b).

70 Existing monitoring programmes are designed to address important questions such as: what is
71 the fate of contaminants (including metals) imported to the site with the disposed material and what
72 effect does this have on ecological components? Associated questions are those relating to the disposed
73 sediments as sources and sinks of metals to the water column, either by diffusion or due to disturbance

74 by storms. At present, the analysis of total metals is the traditional technique used to assess the metal
75 contaminant pressure within the disposal site monitoring programmes. In comparison, little is known
76 regarding metal speciation or detailed vertical distribution and partitioning of metal contaminants
77 between pore-water and solid phases within the sediments at the disposal sites. As such, the impact
78 assessment of disposed material and management accordingly can be limited by using a total metal
79 approach alone in assessing metal pressure within the sediment.

80 The sediment pore-water concentrations of contaminants and hence the bioavailability of
81 chemicals in sediments is often estimated using various techniques (Forstner and Wittman, 1981;
82 Bufflap and Allen, 1995; Stockdale et al., 2009). Pore-water can be obtained by *ex-situ* (slicing,
83 centrifuge, suction, or pressure) methods or *in situ* (probe pumping or diffusion) methods, such as
84 passive samplers (dialysis peepers, teflon sheets, DET and DGT). *Ex-situ* methods are often difficult to
85 control and analyse due to issues in controlling oxidation during sampling, preservation and detection
86 limits associated with small volumes and lack of pre-concentration. Additionally, as samples are
87 handled open to the air, whilst on the boat, issues such as clean handling techniques can be a challenge
88 for standard monitoring conditions. There may also be limitations of sampling resolution (Bufflap and
89 Allen, 1995). Diffusion methods such as passive samplers (Peijnenburg et al., 2014) can be useful in
90 that they can offer high resolution and are constrained inside probes which can allow cleaner handling,
91 without full clean trace metal provisions. Some techniques can also pre-concentrate chemicals which
92 can facilitate analysis success by lowering detection limits. Deployment times are typically ≥ 24 h, but
93 deployments for this length of time can also minimise the effect of disturbances caused by deployment
94 (Davison et al. 2007). Passive sampling methods can provide ‘dissolved’ concentrations in sediment
95 porewater (C_{free}) thus providing a more relevant exposure metric for risk assessment than do total
96 concentrations (Peijnenburg et al. 2014). Other information that can be obtained from passive samplers
97 in sediments includes estimates of metal sources, sinks and time-integrated measurements.

98 Passive samplers such as Diffusive Gradient in Thin Films (DGT) have been used increasingly
99 in sediments to determine pore-water metal ‘dissolved’ concentrations (C_{DGT}) and time-integrated labile
100 metal fluxes (Zhang et al. 1995; Davison et al. 2000; Fones et al. 2001; Fones et al 2004; Peijnenburg
101 et al. 2014; Amato et al. 2015). DGT is a passive sampling technique that has been used for determining
102 metal concentrations in natural waters for more than 20 years (Davison and Zhang; 1994). A typical
103 DGT device for common divalent metal ions consists of Chelex[®]-100 resin embedded within a
104 hydrogel, overlaid with a diffusive layer of hydrogel and a filter membrane. These devices have been
105 successfully employed in the sampling of metals prior to analysis of their concentrations in surface
106 waters (Schintu et al. 2010; Shiva et al. 2016), soils (Oporto et al. 2009; Ernstberger et al. 2005) and
107 sediments (Davison et al. 1997; Fones et al. 2004; Tankere-Muller et al. 2007; Teal et al., 2009; Teal et
108 al., 2013) and by using different binding agents the range of determinands has been extended to include

109 other cations (Dahlqvist et al. 2002), oxyanions (Panther et al. 2014) and targeted species including
110 sulphide (Teasdale et al. 1999) and uranium (Turner et al. 2012; Turner et al. 2015).

111 DGT is a well-developed technique for sampling metals in bulk water, with deployments from
112 6 to 72 h being typical, with the rate of metal uptake by the resin gel controlled by the diffusive layer
113 (Davison and Zhang, 2012). The diffusion coefficient in the diffusive gel is similar to that of the
114 diffusion rate of the metal ion in pure water and can be measured accurately by experiment (Zhang and
115 Davison 1999). Diffusion coefficients for many metals including different species (Metal-NOM
116 complexes) in polyacrylamide gels are available in the literature (Zhang and Davison, 2000; Scally et
117 al. 2006; Shiva et al. 2015). The concentration in the water can then be calculated using the previously
118 published DGT equation (Davison and Zhang, 1994; Davison and Zhang, 2012). One problem
119 associated with this is the potential for metal species and complexes operationally defined as 'labile' to
120 be sorbed onto the resin gel, this thus depends on the relative diffusion rates of the species that pass
121 through the gel (Zhang and Davison, 2000).

122 DGT has also been fully characterized for use in sediments (Zhang et al. 1995; Fones et al.
123 2004; Amato et al. 2014). When used in sediments it is an in-situ technique that provides time-integrated
124 measurements of the combined labile metal fluxes from the sediment pore water and particulate phases
125 (Zhang et al. 1995). Upon deployment of the DGT probe in the sediment, metals dissolved in the pore
126 water are rapidly accumulated on the resin in the binding gel. This generates a localized zone of
127 depletion in the pore waters and induces a release of labile, weakly bound metals absorbed onto
128 sediment particles (Harper et al. 1998; Ciffroy et al. 2011). The DGT device thus acts as a localised
129 sink, removing labile metal species permanently from solution. The metal continuously accumulates in
130 the DGT device while it is deployed in the sediment (Harper et al. 1999) and therefore measures a time-
131 averaged flux from the pore water to the resin (Harper et al 1998 and 1999).

132 Harper et al. (1998) and Zhang et al. (1995) both showed that DGT fluxes can be interpreted as
133 pore water concentrations using Fick's law of diffusion along with metal diffusion coefficients,
134 deployment time and diffusive gel thickness if the metal concentrations at the interface between the
135 DGT device and sediment are well buffered by metal resupply from the sediment solid phase. However,
136 in most cases there is only partial resupply or resupply by metal diffusion so DGT measurements are
137 the result of dynamic equilibriums between the binding strength of the DGT resin and that of the
138 sediment (Davison and Zhang, 2012). Amato et al. (2015) suggested that interpreting DGT
139 measurements as fluxes ($\mu\text{g}/\text{h}/\text{m}^2$) is the most suitable approach for sediment deployments. The DGT
140 metal flux will differ depending on sediment properties and also the chemical behaviour of the metals.
141 These differing release rates will influence accumulation of metals by benthic organisms thus providing
142 the use of DGT-metal fluxes for assessing metal bioavailability in sediments (Simpson et al., 2012;
143 Amato et al. 2014; Amato et al. 2015). However, only a few studies have utilised DGT sediment

144 measurements in the context of contamination studies at capping (Knox et al., 2012; Knox et al., 2016)
145 or disposal sites.

146 While the established practise of analysing total trace metals in bulk sediment samples gives
147 important information about absolute concentrations and so potential hazards, looking at depth resolved
148 profiles of metal fluxes as measured by DGT improves our understanding of how mobile and thus
149 available these metals are from a total disposal reservoir. In other words, what actual risk disposed
150 sediments pose. The bioavailability of heavy metals has been more closely linked to levels of dissolved
151 contaminants in pore-waters than to bulk sediment concentrations (Calmano et al., 1993; Ankley et al.,
152 1996b; Chapman et al., 1998; Eggleton and Thomas, 2004) as bioavailability and toxicity of metals in
153 sediments was not well predicted by sediment metal concentrations only (Lee and Lee, 2005).

154 The aim of this work was to apply therefore a passive sampling approach, diffusive gradient in
155 thin films (DGT) technology, as a complementary tool to the routine monitoring conducted at an UK
156 disposal site and thus assess the additional insight and understanding of metal behaviour and fate gained
157 by including this technique in a monitoring programme. Some of the metals examined (lead, nickel and
158 cadmium) are on the EU Water Framework Directive (WFD) list of priority substances and OSPAR list
159 of priority pollutants while others have mainly ecological relevance (iron and manganese).

160

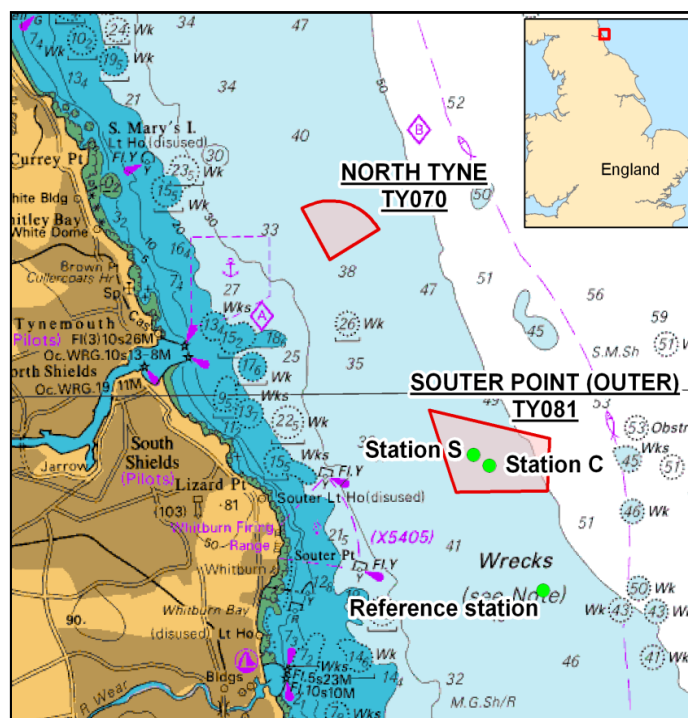
161 **2.0 Materials and methods**

162 *2.1 Study site*

163 The Souter Point disposal site is located off the North East coast of the UK (Figure 1). This site has
164 been used for the disposal of dredged material since 1952 and selected stations have been monitored
165 annually since the early 1970s (Bolam et al., 2010a; Bolam et al., 2010b). The site is located at a depth
166 of approximately 40-50 m, shallowing by up to 5m towards the western boundary due to historical
167 accumulations of minestone and fly-ash deposits (Rees et al., 2006). Tidal currents in the vicinity of
168 the disposal site are moderate in strength and run generally parallel to the coastline, with a southerly
169 net residual drift. The sediments within the vicinity of this disposal site are muddy sands. However,
170 sediments may vary to a large extent following dredged material disposal and in relation to a sites earlier
171 history of solid industrial wastes and other discharges inshore (Rowlatt, et al., 1989; Rowlatt and
172 Ridgeway, 1997; Birchenough et al., 2007). The results of this work summarises results obtained during
173 a research cruise conducted in June 2011. Observations and measurements were made during the cruise
174 and on recovered samples back at the laboratory.

175 *2.2 Sampling approach*

176 A 0.1 m² NIOZ box-core was used to collect sediment at 3 stations: 4 core replicates were collected
177 from the Reference station (located to the south of the disposal site) and 3 core replicates were taken
178 from each of stations C and S, both located within the disposal site (Figure 1).



179

180 Figure 1. Souter Point disposal and sampling stations on the disposal stations (S, C) and reference
 181 station (R).

182

183 The DGT devices for metals in sediments were purchased as complete assembled probes from DGT
 184 Research (Lancaster, UK). The overall dimensions are 5 x 240 x 40 mm, with an exposure window of
 185 18 x 150 mm and the device consists of a 0.8 mm APA diffusive gel, polyethersulphone filter membrane
 186 and Chelex binding layer. Probes and procedural blanks were de-oxygenated in a 0.01M NaCl solution
 187 overnight using oxygen free-nitrogen. The cores were placed in an incubating tank (in the dark and
 188 filled with oxygenated seawater) on-board ship and were stabilised for 2 hours before deployment of
 189 the probes. For each core, two probes were used: the Chelex gel probe (for metals determination) and
 190 the silver-iodine (AgI) gel probe (for sulphide determination). The probes were inserted into the
 191 sediment core, leaving 1 - 2 cm between the top of the probe window and the sediment/water interface.
 192 Furthermore, Chelex gel discs and AgI gel discs were deployed in the incubating tank in parallel with
 193 the probes to determine concentrations in the overlying water column. The probes and discs were
 194 deployed for 24 - 28 hrs. The time and temperature were recorded at the deployment and retrieval
 195 points. On removal, nanopure water (resistivity of 18.2 MΩ·cm) was used to rinse off any sediment
 196 traces that remained on the surface of the probes/discs. These were stored in a labelled bag and kept in
 197 the refrigerator prior to transfer to the laboratory for analysis.

198 Five replicate Sediment Profile Imagery (SPI) images were taken at each of the sites where the
 199 DGT technique was employed. Sediment Profile Imagery is a rapid, *in-situ* technique, which takes
 200 vertical profile pictures of the upper 20cm of the sediment system. The SPI camera works like an

201 ‘inverted periscope’, the camera possesses a wedge-shaped prism with a Plexiglas faceplate and an
202 internal light provided by a flash strobe. The back of the prism has a mirror mounted at a 45° angle
203 which reflects the image of the sediment-water interface at the faceplate up to the camera. The imaging
204 system (a Nikon D-100 camera) provides *in-situ* visualisation of sediment characteristics (layers,
205 structure) and the interaction of the sediment and succession of large in-fauna (Rhoads and Germano,
206 1982; Germano et al., 2011). Visual assessment of sediment colour can be used to assess sediment redox
207 state, in particular iron reduction (loss of brown), manganese reduction (grey) and pyrite formation
208 (black), (Lyle, 1983; Bull and Williamson., 2001; Teal et al., 2009; Teal et al., 2010).

209

210 2.3 Analysis of passive samplers

211 *Chelex gel*: The DGT probes were rinsed with nano-pure water once retrieved. After opening the
212 window frame, the filter and diffusive gel layer were removed and discarded. The remaining resin gel
213 layer was carefully placed on a flat surface and the gel was sliced at 0.5 cm resolution. Each slice was
214 then placed in a sample tube and 1 ml of 1M HNO₃ was added to the tube, ensuring that the resin gel
215 layer was fully immersed in the HNO₃ solution. The sample was left to elute for at least 24 hours before
216 analysis (Davison *et al.*, 2007). The eluted solution was then diluted prior to analysis by Inductively-
217 Coupled Plasma-Mass Spectrometry (ICP-MS) using an Agilent 7500ce (Agilent Technologies,
218 Waldbronn, Germany), and by Inductively-Coupled Plasma-Atomic Emission Spectroscopy (ICP-
219 AES) using a Varian Ax Vista Pro (Agilent Technologies, Waldbronn, Germany). Quantification of
220 Cd, Fe, Mn, Ni, and Pb was performed by external calibration and deploying eight levels (0, 0.5, 1, 5,
221 10, 20, 100 and 500µg/L) of working standard solutions which were prepared from a customised mixed
222 metal standard solution of 100mg/L (SPEX Certiprep Ltd, Middlesex, UK). The limits of quantification
223 (LOQ) for each metal DGT analysis (24hr deployment) are (nmol/cm²/s): Cd; 2.8x10⁻⁸, Pb: 1.14x10⁻⁸,
224 Ni: 5.7x10⁻⁸, Fe: 9.7x10⁻⁶, Mn: 1.6x10⁻⁷.

225

226 *AgI gel*: The AgI gels were removed from the probes and covered with a polyester film. The gels were
227 then scanned while wet in a flat-bed scanner. The greyscale intensity of the scanned images was
228 analysed with the software Image J (<http://rsb.info.nih.gov/ij/>). Using the calibration curve derived by
229 Teasdale *et al.*, 1999, total dissolved sulphides can be quantitatively measured in the gel.

230

231 *Metal flux calculations*: The measured concentrations, C_g (µg kg⁻¹) of the DGT gel solutions were
232 converted to molar concentrations and used to calculate the mass, M (nmol cm⁻²), accumulated in the
233 resin layer of each gel strip:

234

$$235 \quad M = \left(\frac{C_g (v + V)}{0.8 \times A} \right) \frac{1}{x} \quad (1)$$

236 where V is the volume of gel (mL), v the extractant volume (mL) and x the atomic mass of the element
237 in question. The factor 0.8 accounts for the fact that only 80% of the bound metal is released (Davison
238 et al. 2000). Knowing the time of gel deployment, t (sec), allowed calculation of the time averaged Flux
239 F ($\text{nmol cm}^{-2} \text{s}^{-1}$) of metal from the porewaters to the resin strip,

240

$$241 \quad F = \frac{M}{t \times A} \quad (2)$$

242

243 where A is the area of exposed gel (cm^2). The term ‘flux’ used from here onwards thus refers to the flux
244 of reduced metal forms from the pore water to the resin gel of the DGT device, here onwards referred to
245 as ‘resin gel’ (i.e. not reduction fluxes or process rates) and serves as a proxy for metal availability.

246

247 *2.4 Supporting sediment analysis*

248 Supporting measurements to complement the DGT probes and characterise the sediment at each of the
249 stations were also collected. Oxygenation of the upper sediments layer was measured using oxygen
250 pore water profiles obtained on intact cores and using oxygen microelectrodes (Unisense, Denmark)
251 and a method adapted from Rabouille et al. (2001). Sediment characteristics were derived from vertical
252 slices of sub-cores from a NIOZ box-corer at resolutions 0 to 0.5 cm, 0.5 to 1 cm and then at 1 cm
253 intervals, stored at -20°C or analysed immediately. These sample slices were analysed for particle size,
254 porosity, chlorophyll/phaeopigment and total organic carbon content.

255 Particle size analysis (PSA) was conducted using a method developed by Mason et al. (2011).
256 In short, a subsample of each sediment was screened at 1 mm and laser sized using a Malvern
257 Mastersizer 2000 (Malvern, Worcestershire, UK). The remaining sample was wet split at 1 mm, and
258 the > 1 mm sediment was oven dried and then dry sieved over a range of test sieves down to 1 mm.
259 Sediment < 1 mm was oven dried and weighed. The results from these analyses were combined to
260 provide a full particle size distribution. Summary statistics, including % gravel, % sand and % mud,
261 were derived from the full distribution dataset. Total Organic Carbon (TOC) was analysed using broadly
262 similar methodology to that described by Verardo et al., 1990. Samples were freeze-dried and then
263 ground to homogenise the sample. Inorganic carbonate was removed from a 1.3 g subsample using
264 sulphurous acid to excess. Sub-samples (~ 0.5 g) were then weighed into tin cups and analysed using a
265 Carlo Erba EA1108 Elemental Analyser. Chlorophyll a and phaeopigments were extracted in 90%
266 acetone (Fisher Scientific, Leicestershire, UK) and refrigerated before analysis. A Turner Designs
267 Model 10AU filter fluorometer (Turner Designs, Sunnyvale, California, USA) was used to measure
268 extracted chlorophyll a by fluorescence before and after acidification, as described in Sapp et al. 2010.
269 The fluorometer was calibrated using a solution of pure chlorophyll a (Sigma-Aldrich, St. Louis) with
270 the concentration being determined spectrophotometrically. The percentage error of chlorophyll a
271 analyses was $< 2\%$ relative to Turner-certified reference material. Porosity was calculated using the

272 dry weights and wet weights of known volumes of sediment slices assuming a sediment particle density
273 of 2.7 g cm^{-3} and a seawater density of 1.035 g cm^{-3} (Sapp et al. 2010).

274

275 *2.5 Total Metals*

276 A sub-core from each station was taken and sliced according to its visual description. Each slice was
277 subsequently analysed for total metals on the $< 63 \mu\text{m}$ sediment fraction. Typically, 0.2 g of the sieved
278 and freeze-dried sediment sample was digested in a mixture of hydrofluoric (HF), hydrochloric and
279 nitric acids using enclosed vessel microwave heating. The HF was then neutralised by the addition of
280 boric acid and the digest made up in 1 % nitric acid and further diluted prior to analysis by ICP-MS and
281 ICP-AES. Quantification of Cd, Fe, Mn, Ni, and Pb used external calibration with Indium as internal
282 standard. A method blank and a certified reference material (CRM) PACS-2 (a marine sediment
283 produced by the National Research Council Canada) were run within each sample batch so that the day-
284 to-day performance of the method could be assessed. Shewhart control charts were derived from the
285 CRM data and monitored using (upper/lower) warning and control limits set at ± 2 and 3 standard
286 deviations from the mean value, respectively. Any batches with results outside these control limits were
287 rejected and the samples re-analysed. The mean recoveries of all elements of interest range from 94%
288 to 116% with a % relative standard deviations ranging from 2.8% to 12.2%.

289

290 *2.6 Statistical approaches and analysis*

291 To aid in comparing and contrasting features of DGT profiles within and between sites, a statistical
292 model was fitted to each of the metal profiles. Before the main analysis, mean values were taken over
293 the replicates to avoid statistical complications caused by spatial correlations between the cores. When
294 examining the profiles, natural logs (Ln) were taken to reduce the visual impact on the profile of large
295 readings. The Ln data also better fitted the assumptions behind the modelling which followed.

296 Initially, Ln profile plots of all eight metals were completed at all sites. For metals exhibiting the biggest
297 differences between sites (Pb, Ni, Mn and Fe), further modelling was conducted to tease out the
298 statistical evidence for these differences. We describe this modelling below.

299 The depth profiles for each of the metals at the three stations was smoothed using a Generalised
300 Additive Model (GAM) (Wood, 2006) using the R package mgcv (R Development Core Team, 2010).
301 Thin plate regression splines were used to smooth the data and the degree of smoothing (number of
302 degrees of freedom (df) for the model parameters) was set to the minimum needed to explain the main
303 fluctuations in the profile: we used 5 df for Pb and Mn and 4 df for Ni and Fe. The residuals (data minus
304 the smoothed value) were calculated at each of the observed depths. For Pb and Ni, autocorrelation
305 plots suggested that neighbouring residuals were independent; however, residuals from the Mn and Fe
306 profiles were correlated. Thus, two different kinds of models, one assuming independence and one
307 assuming one-lag auto correlation were required to model the depth profiles.

308 For the independent residuals, for a particular site and at each depth i , we assume that data arises from
 309 the model:

$$310 \ln(M_i) = s_i + e_i \quad (3)$$

311 where s_i is the smoothed value from the GAM model of metal M_i , and e_i is an independent error term
 312 which we assume to be distributed $N(0, \sigma^2)$, where σ^2 is the variance of points around the smoothed
 313 line σ^2 is estimated by the sum of the squared residuals divided by $(n - k)$, where n is the number
 314 of points and k is the number of degrees of freedom used in fitting the GAM model.

315 For the autocorrelated models, an autoregressive model of order 1 was used to the model the residuals:

$$316 r_i = \alpha r_{i-1} + e_i \quad (4)$$

317 where r_i is the i th residual, α is a parameter (estimated by maximum likelihood using the *ar* function
 318 in R) and e_i is an independent error term as in model (3). Simulated realisations of M_i were generated
 319 from (4) by adding on the smoothed surface s_i .

320 One thousand realisations were then simulated from the model in (3) or (4) and the mid 95% envelope
 321 taken. This is equivalent to a 95% confidence interval for the profile at each depth (Manly, 2008).

322

323 3.0 Results and discussion

324 3.1 Bulk metal and sediment characteristics

325 A summary of station sediment characteristics is shown in Table 1a and b and Figure 2 and bulk
 326 sediment metal profiles are illustrated in Figure A.1 (Appendix 1).

327

328 Table 1a: Mean sediment characteristics from sliced sediment cores (0 to ~10cm). Number in brackets
 329 is one standard deviation.

330

Station	Silt/clay ($<63 \mu\text{m}$, %)	Porosity	Chlorophyll (mg/m^3)	Phaeo- pigment (mg/m^3)	TOC (% mass/ mass)	Oxygen penetration (OPD) - cm
Reference	17.0 (3.7)	0.45 (0.04)	3.0 (2.3)	14.0 (7.0)	1.3 (0.3)	0.5 (0.2)
Disposal S	49.2 (20.7)	0.62 (0.05)	3.4 (2.4)	14.2 (6.9)	5.6 (1.6)	0.4 (0.2)
Disposal C	22.4 (16.9)	0.53(0.05)	4.7 (3.9)	14.7 (7.4)	5.4 (0.9)	0.4 (0.1)

331

332

333

334

335

336

337

338

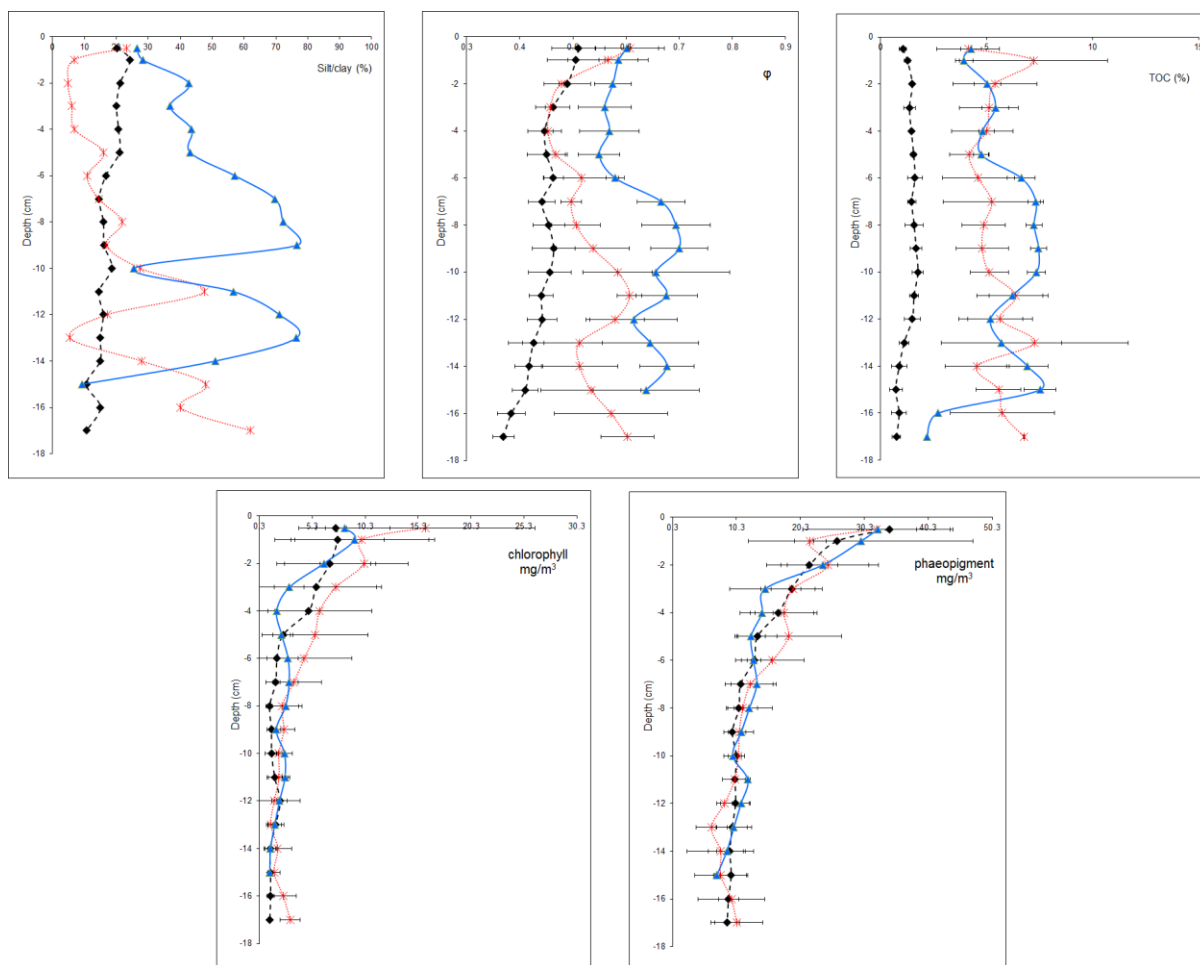
339

340 Table 1b: Mean total metal concentration from bulk samples from core layers (full plots are in Appendix
 341 1 Figure A.1)
 342

Average Concentrations [#]	Ni (mg/kg)	Cd (mg/kg)	Pb (mg/kg)	Mn (mg/kg)	Fe (g/kg)
Reference (n=4)	50.0	<0.18	136	445	38.9
Disposal C (n=7)	49.6	0.50	172	510	39.6
Disposal S (n=6)	50.6	0.46*	164	475	39.1

343 *Cd at layer 8-9cm <0.2mg/kg

344 [#]SD not available as single measurement at each layer.



345

346 Figure 2: Vertical profiles of sediment properties at the three stations (reference, station C and station
 347 S) Silt/clay (%), Porosity, Total Organic carbon (%m/m), Chlorophyll and
 348 Phaeopigment. Error bars are +/- 1 standard deviation, n=3

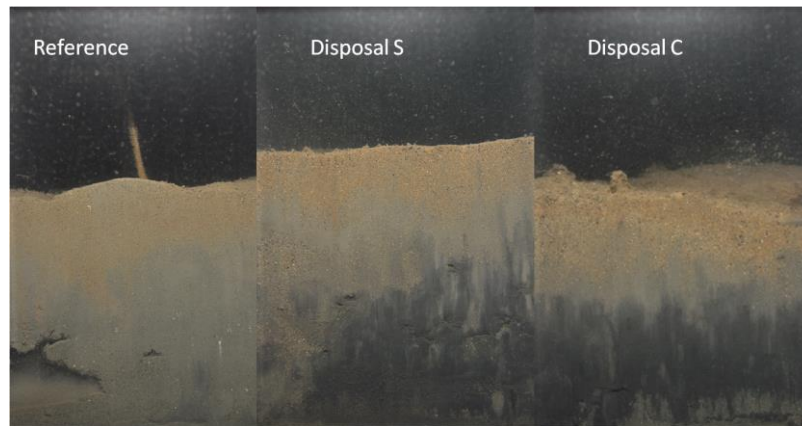
349

350 All stations were composed of either muddy sands where the sand:mud (mud being defined as the
 351 sediment fraction $<63\mu\text{m}$, and sand between $63\mu\text{m}$ and 2mm) ratio is $>1:1$ and $<9:1$; or to a lesser extent
 352 sandy muds, where the sand:mud ratio is $>1:9$ and $<1:1$; as defined in Folk classification (Folk, 1954).
 353 Note all bulk samples contained $<2\%$ gravel and therefore for the purposes of these descriptions this
 354 has been ignored. Porosity in the upper layers of the sediment at the reference station was lowest (0.45)
 355 and elevated at the disposal stations, especially in the deeper sediment layers. Total organic carbon was
 356 lowest at the Reference station with higher total organic carbons ($> 5\%$ m/m) at the two disposal
 357 stations. The sediment characteristics depth profiles (Figure 2) illustrate the differences between the
 358 reference and disposal stations. The reference station showed a gradual decrease in porosity and organic
 359 carbon with depth whilst the disposal stations exhibited complex porosity and carbon signatures down-
 360 core probably related to disposal events. The heterogeneous structure in vertical profiles illustrated the
 361 contrasting disposal events at the impacted stations at different depths and with differing % silt/clay,
 362 TOC and porosity signatures. Station C in particular exhibited a low % silt/clay level in the upper parts
 363 of the sediment. The pigment profiles are similar across the stations and illustrate the water column

364 source with similar degradation profiles with depth. The oxygen profiles and penetration depth were
365 similar for all the stations, with diffusion-type profiles and with oxygen consumed within the upper 1 cm
366 of the sediment. Observations conducted on the SPI images using Fe^{3+} colour also showed that more
367 reduced sediment conditions were found deepest at the reference station, and shallowest at the disposal
368 stations (Figure 3). The SPI images also showed the occurrence of sulphide formation (black
369 colouration) to be more intense and shallower in the disposal station sediments when compared to the
370 reference station and this supports an assessment of increased reducing conditions at these sites.

371

372



373

374 Figure 3: Example Sediment Profile Images (SPI) from the three stations at Souter Point (size of SPI
375 optical window is 15 cm wide by 20 cm deep).

376

377

378 *3.2 DGT fluxes and profiles*

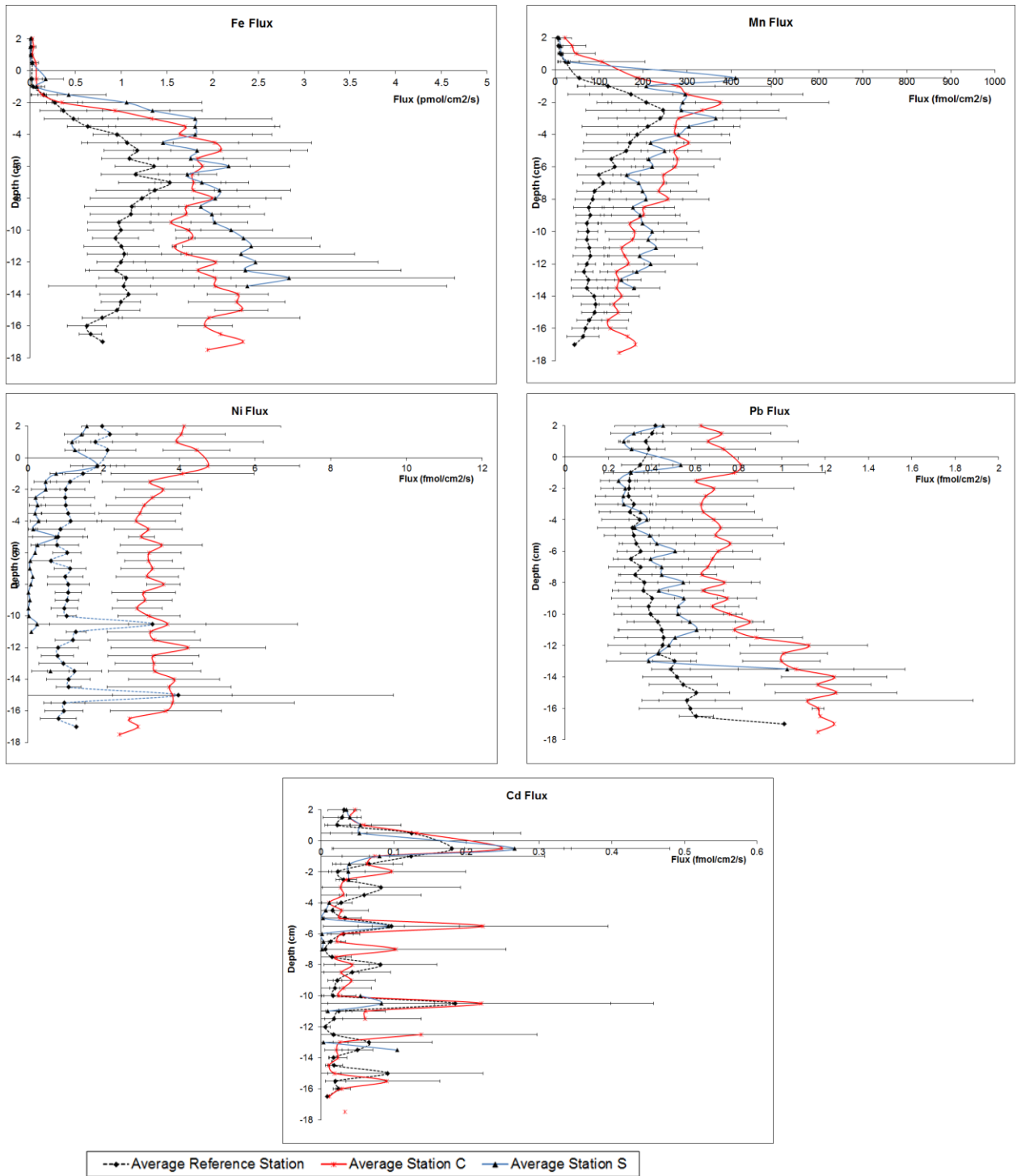
379 DGT metal fluxes were calculated for each of the deployed DGT probes at each station according to
380 the method described in Davison and Zhang (1994) and the average flux profiles (\pm sd) were plotted
381 for each metal at the 3 stations (Figure 4).

382

383 *3.3 Metal sediment behaviour*

384 **Iron and Manganese:** The DGT flux profiles showed high resolution information of iron (Fe) and
385 manganese (Mn) remobilisation behaviours. Both metals are redox sensitive and are used as successive
386 Terminal Electron Acceptors (TEAs) during the remineralisation of organic matter, Mn before Fe
387 (Burdige, 2006). Their supply to the resin gel increased as they became reduced in the sediments (Fe^{3+}
388 to Fe^{2+} , Mn^{4+} to Mn^{2+}). Consistent with this, Fe and Mn DGT flux profiles (Figure 4) showed the start
389 of sub-surface remobilisation at about 1 – 2 cm and < 1 cm, respectively. Mn release occurred as oxygen
390 was depleted within the upper centimetre of the sediment. Iron supply to the resin gel rapidly increased
391 near the surface, but below the oxic zone. This close linkage between Fe and Mn behaviour and
392 oxic/suboxic carbon remineralisation processes is usual in marine sediments (Burdige, 2006; Gao et al.,
393 2009; Teal et al., 2009; 2013). Increasing DGT-iron fluxes near the sediment surface occurred at all

394 stations and there was continued supply to the resin gel at increasing depths. The rate of increase of iron
395 supply with depth at the disposal stations was greater than at the reference station and is likely to be
396 driven by the more reducing conditions found at these locations. Iron showed continued supply to depth
397 whilst Mn showed a subsurface peak.



399

400

401

402 Figure 4: Vertical profiles of metal flux to the DGT probes at the three stations (reference, station C
 403 and station S) - Fe, Mn, Ni, Pb, Cd. Error bars are +/- 1 standard deviation, n=3

404

405 The peak in the Mn concentration in the subsurface layer is often observed in coastal systems (Gao et
406 al., 2009; Teal et al., 2013), however, the continued supply of iron to the resin gel with increasing depth,
407 found in this study, is in contrast to others which show an iron peak (Gao et al., 2006; Merritt and
408 Amirbahman; 2007). This continued supply at depth could be linked to very low sulphide
409 concentrations which allow reduced iron to be readily available for uptake by the DGT probes. The
410 supply rates for Fe and Mn to the resin gel from sediments at the disposal stations were higher than at
411 the reference station. This is consistent with the higher organic matter loads at the disposal sites and
412 thus the increased reducing conditions found there. This is also corroborated by the SPI images at the
413 disposal sites, which show more reducing conditions closer to the sediment surface. The Fe fluxes were
414 one order of magnitude higher than Mn fluxes. The profile shapes indicate a supply of dissolved Mn
415 across the Sediment – Water Interface (SWI) into the water column, but this was not observed for iron,
416 which is probably oxidised within the upper cm of the sediment where oxygen is present. The DGT flux
417 profiles indicate that the resupply to the resin gel is higher at the disposal sites, despite similar bulk Fe
418 and Mn levels across the sites.

419

420 **Cadmium:** All 3 stations showed a peak of DGT available cadmium at the SWI. Below the SWI, levels
421 of Cd supply were low at all stations, apart from distinct peaks of higher Cd supply at discrete depths
422 (0.1 to 0.2 fmol/cm²/s). This release of Cd across the SWI and the maximum in the sediment surface
423 layer can be attributed to the mobilisation of metal from particles having recently been deposited on the
424 sediment surface, mainly through the rapid degradation of organic matter accumulated on the surface
425 of the sediment. This process can be related to break-down of deposited phytodetritus (Fones et al.,
426 2004; Sakellari et al., 2011) and can also be associated with other metals such as Cu and Zn. There was
427 no trend of Cd release with increasing depth at any of the stations. The low Cd particulate concentrations
428 and lack of difference in Cd supply between the reference and disposal stations would imply that Souter
429 Point stations were not a significant source of Cd release into the pore-water associated with dredged
430 material disposal, but that it is likely that the SWI Cd source was seasonal deposition and burial of
431 phytodetrital material.

432

433 **Lead:** Lead (Pb) profiles showed increasing flux to the resin gel with depth, with the flux rate increasing
434 at all stations in the deeper sediment layers. The fluxes at the reference station and at the disposal station
435 S were similar, whilst disposal station C showed the highest Pb fluxes (Figure 4).

436 The variability (relative SD) in Pb flux with depth was lower at the reference station and highest at the
437 disposal stations. This variance was similar to other metals, illustrating the heterogeneity in sediment
438 conditions and hence metal cycling introduced by dredged material disposal operations. The levels of
439 total Pb were highest at the disposal station C, but not directly proportionate to the much higher supply
440 rates observed. This discrepancy showed that mechanisms of metal release could be complex and
441 therefore cannot be determined from total sediment metal content alone. Indeed, studies have shown

442 that Pb could respond much more to concentrations of organic matter and Acid Volatile Sulphide (AVS)
443 (Duran et al., 2012) rather than other sediment variables. Both disposal stations show a surface peak in
444 Pb supply to the resin gel close to the SWI which means that these sites could be acting as sources of
445 pore-water Pb to the water column. This is not the case at the reference station. It is possible that this
446 release of Pb (a metal with a high partition co-efficient, K_d) within the upper layers of the sediment
447 could be linked to Fe/Mn particulate reduction. In sub-oxic zones within estuarine sediments, Fe and
448 Mn can act as master variables controlling the distribution and speciation of other trace elements
449 (Forstner et al., 1986; Butler et al., 2005).

450

451 **Nickel:** All 3 stations showed an increase in nickel (Ni) supply to the DGT device in the upper few cm
452 of the sediment, with consistent supply rates at depths greater than 5 cm. This increase is likely to be
453 linked to the reduction of Fe and Mn oxyhydroxides and degradation of organic material as shown by
454 the Fe/Mn flux and labile carbon (chlorophyll/phaeopigment) profiles. This behaviour has also been
455 observed in other DGT studies (Tankere-Muller et al., 2007). The overall supply of Ni to the sediment
456 pore-water throughout the profile at disposal station C was higher than at the other two stations. It is
457 likely that the presence/absence of other complexing species (not sulphides) must be creating this
458 between station heterogeneity of supply to the resin gel, given the consistent total Ni particulate pool.

459 Similar to the observed Pb behaviour, the release of Ni near the SWI can be a source of Ni to
460 the water column. This was observed at both disposal stations, in contrast to the reference station. For
461 Ni this could be driven by local release to pore-waters in the upper layers of the sediment (0 to 5 cm
462 depth).

463

464 **Sulphide:** Metal availability and mobility can be closely linked to the amount of free sulphide ions in
465 sediments, especially at depth (Gao et al., 2009). Deployment of AgI gel probes into the sediments cores
466 revealed that free sulphide was at or below the limit of detection for the DGT based method evaluated
467 through colour scanning. The sulphide detection limit for the AgI gels was 0.25 $\mu\text{mol/L}$ for a 24 hour
468 deployment which equates well to previous studies (Teasdale et al., 1999). This correlated well with
469 the high concentrations of free Fe and Mn ions observed in the metal profiles, as any free sulphide
470 would have reacted with the Fe and Mn to form insoluble iron/manganese-sulphide complexes.

471

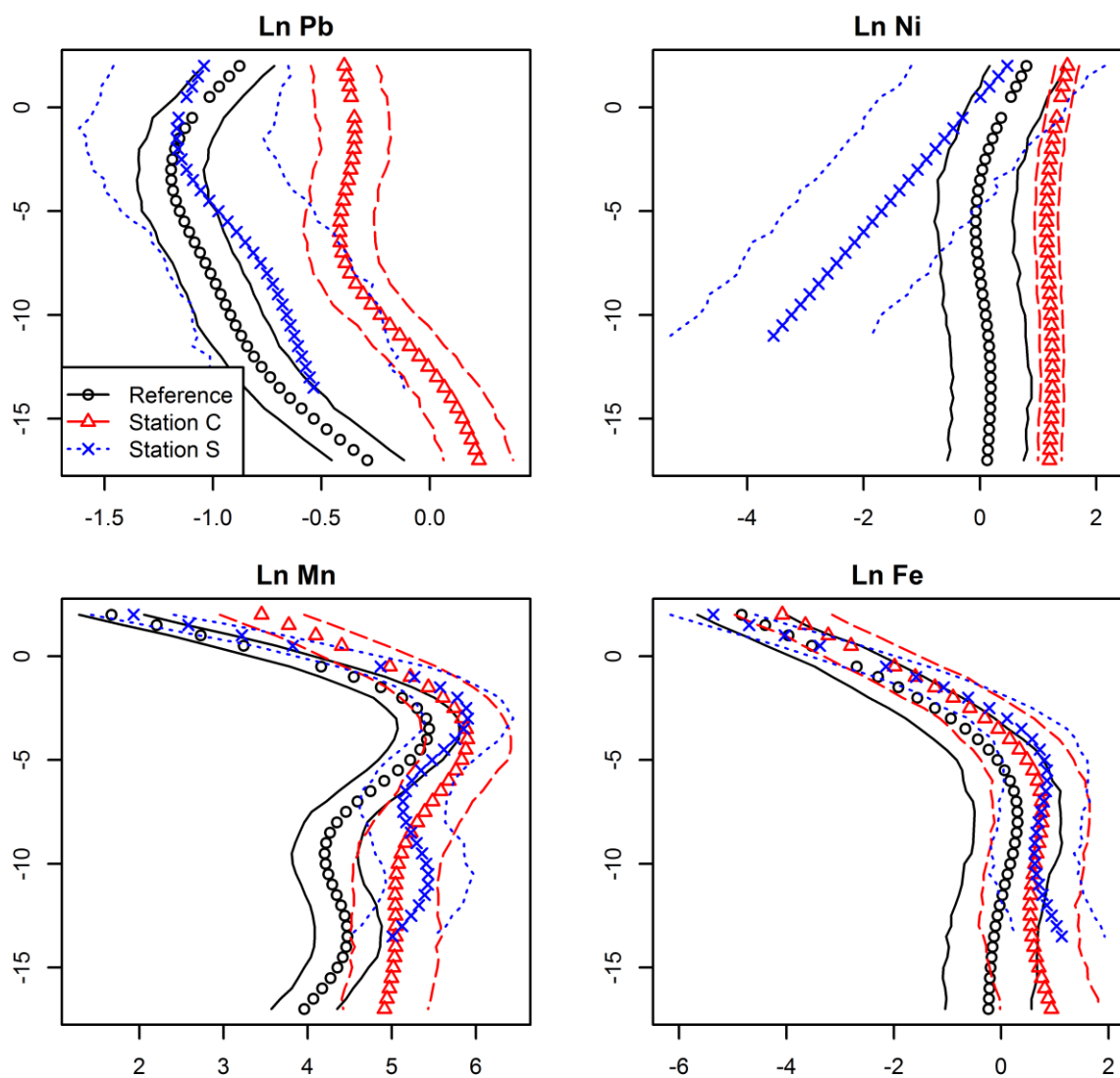
472 *3.4 Statistical analysis and comparison of the DGT profiles*

473 Figure A.2 (Appendix 1) shows natural log depth profile plots for all five metals. For Cd, it is difficult
474 to statistically distinguish the profiles between the stations. For the remaining four metals (Pb, Ni, Mn
475 and Fe), we used the 95% envelope plots in Figure 5 to further explore differences between the sites.

476 For Mn and Fe we used the 1-lag autocorrelation models (equation (4)) for the residuals to create these
477 envelopes (see Figure A.3, as an example, to see the autocorrelated residuals for Mn). Note that these

478 models did successfully remove the autocorrelation. For Pb and Ni we used the independence model in
479 equation (3).

480 For Fe, the envelopes overlap throughout the profile and it is impossible to distinguish the stations from
481 each other. In contrast, the Ni reference and station C profiles are consistently different, whereas the
482 station S profile diverges from the other two with increasing depth. Stations S and C (the disposal
483 stations) have similar profiles for Mn, but the reference station profile separates off slightly from the
484 other two at depths below about 8cm. The reference and station C profiles are very different for Pb.
485 However, the large amount of variation for station S makes it difficult to distinguish this station from
486 the other two statistically.



487
488 Figure 5: 95% confidence envelopes for the profiles of Ln metal flux to the passive sampler at each
489 station for Pb, Ni, Mn and Fe

490 In summary, for Mn and Fe the reference station profile is statistically different from the other
491 two stations, especially at depth, whereas it is difficult to distinguish between the profiles for the other

492 two disposal stations (S and C). For Pb, as previously seen, station C is distinctly different from the
493 other two stations whereas there is only an obvious difference between profiles for site S and the
494 reference station at mid depths. For Ni all three stations are different for almost the whole profile with
495 the reference fluxes lying between lowest fluxes at station S and highest fluxes to the resin gel at site
496 C. The only exception is near the surface, where station C and the reference station have similar profiles.

497 This analysis is designed to introduce some statistically defensible method to describe and test
498 differences between DGT profiles in relation to different metals, sites and the impact of an activity such
499 as dredge material disposal. This can be very useful for regulatory or licensing purposes in comparing
500 spatial or temporal changes in metal behaviour. The work here illustrates that given the high variability
501 within some sites it can be difficult to determine statistically the difference between disposal and
502 reference stations for some metal fluxes. Greater replication (here $n = 3$ at each station) would improve
503 the power of such a technique, helping to distinguish reference and impact changes in sediment
504 conditions for improved disposal site monitoring (over different depth or spatial and temporal
505 resolutions).

506

507 *3.5: Summary of findings and discussion*

508 Dredging and disposal are major activities for sustainable port development and expansion worldwide.
509 The assessment of the effects of sediment metal contamination, associated with dredging and disposal,
510 on biological assemblages and function remains a key question in marine management. However, the
511 appropriate description of bioavailable metal concentrations within pore-waters has rarely been
512 reported, as routinely only total metal concentrations are monitored. In the majority of targeted
513 monitoring programmes, where cost-effectiveness and increasing complexity of regulatory questions is
514 an ever increasing demand, there is an opportunity to incorporate novel approaches which can improve
515 the information and understanding provided. For example, changing regulatory demands from
516 understanding metal contamination levels towards biological effects/toxicity and impact assessment
517 and human activity management. In this work we have attempted to test the use of DGT passive sampler
518 as means of generating cost-effective (compared to conventional porewater sampling, total metal
519 analysis at an equivalent resolution or specific bioavailability studies), targeted and novel information
520 on metal release (sources and sinks) and behaviour within marine sediments.

521 Traditional monitoring of disposal sites within the UK provides the quantitative analysis of total
522 metal within bulk sediments with limited depth resolution (see Appendix 1 Figure A.1). This is used to
523 undertake assessments of metal risk posed from a total pool. Many papers have illustrated the lack of
524 agreement between total metal concentrations and metal availability in the pore-waters and hence
525 bioavailability and ecotoxicological risk (Di Toro 1992; Lee and Lee, 2005; U.S. EPA, 2005; Roullier
526 et al., 2008). In comparison, the DGT technique applied in this study has provided higher resolution
527 depth information on comparative fluxes of metals to the pore-water (primarily via dissolution and/or
528 desorption of weakly bound metals from the solid phase), and hence potential bioavailability (via

529 various solute pathways). This type of information can describe areas of metal loss/remobilisation with
 530 depth, contrast the release/resupply of metals between sites and can also illustrate the presence,
 531 magnitude and direction of metal fluxes across the sediment-water interface. Table 2 summarises each
 532 of these information types supplied by the DGT (namely, metal behaviours observed at the three sites
 533 with respect to DGT, Sediment-Water Interface fluxes, and additional information supplied by DGT)
 534 in comparison to the total metal enrichment information. The implications of these findings are
 535 discussed further in subsequent sections.

536

537 Table 2. Summary metal behaviour at the 3 disposal site stations as derived by DGT profiles and
 538 comparison to total bulk metal reservoir (SWI = sediment-water interface)
 539

Metal	Enriched in disposal sediments	Depth profile shape and flux to DGT	Flux across SWI	Insight given by DGT profiles
Ni	No	Shallow sub-surface peak of Ni release at disposal sites only. Supply to resin gel consistent with depth across all sites. Flux to resin gel higher at station C.	Flux to water column at disposal sites, associated with a shallow sub-surface peak.	Supply of Ni to water column at disposal sites. Pore-water chemistry controls supply to resin gel at station C.
Cd	Yes	Shallow subsurface peak (<1cm) at all sites. Distinct peaks of remobilisation and flux to resin gel. Some LOQ issues. Not coupled to total sediment metal (bulk or profile).	Flux to the water column at all stations, associated with shallow sub-surface peak.	Release not linked to disposal source. Likely phytodetritus source but controls related to redox (Fe/Mn).
Pb	Yes	Increased supply to resin gel with depth. Flux to resin gel significantly higher at station C.	Flux to water column at disposal sites, associated with a shallow sub-surface peak (Pb release from Mn/Fe reduction).	Higher disposal total metal only released at station C. Other factors controlling DGT uptake (S^{2-} , DOC). Link to Mn or Fe particulate reduction ~ high Pd Kd
Fe	No	Increased Fe supply to resin gel below oxic layer (>1cm). Rate of increase and flux greater at disposal sites. Flux is maintained or increases with depth.	None – oxic layer prevents release.	Higher iron release at disposal sites – linked to increased reducing conditions at depth & elevated TOC. No SWI exchange limited by oxic layer
Mn	Yes	Increased resupply as oxygen saturation decreases.	Flux to the water column at all sites	Release governed by increasingly reducing

	Peak resupply in upper 4 cm and then decline to depth. Flux to the resin gel and depth/rate of increase with depth is higher at the disposal sites.	but higher at disposal sites.	conditions at disposal sites (fines and TOC).
--	---	-------------------------------	---

540

541 *Metal behaviour (release, availability, cycling) information provided by DGT:*

542 Firstly, DGT provides high resolution information with depth DGT flux data inferred to be
543 DGT-labile metal (dissolved metal present in the pore-water as well as “weakly” bound to the solid
544 phase), its production within the sediment, release and behaviour, and associated site differences. Iron
545 and manganese display behaviour consistent with increasingly reducing conditions at depth, i.e.
546 increased release to the pore-water and availability to DGT. Two of the metals (Pb, Ni) illustrate
547 subsurface DGT-labile (C_{DGT}) peaks (close to the SWI ~ <1cm) which can be a result of increased metal
548 release from degradation of organic material and/or reduction of Fe and Mn oxyhydroxides associated
549 with elevated TOC loading associated with disposal activity (i.e. only present or elevated at the disposal
550 sites). Thus, these disposal sediments represent a source of metal to the overlying water column.
551 Additionally, the overall increase of metal fluxes observed across the whole sediment profile for Ni and
552 Pb in the disposal sites (especially in site C) could be evidence that the disposed sediment material may
553 release larger amounts of DGT-labile (and hence bioavailable) metals in the pore water.

554 Although Cd exhibits similar peaks of DGT flux (DGT-labile metal), the magnitude and depth
555 distributions of the DGT-Cd fluxes are similar across all sites, despite the elevated bulk total Cd levels
556 reported at the disposal sites. It is therefore likely that this Cd supply to the pore-water is not related to
557 disposal activities, but decomposition of Cd enriched phytodetritus, either at the surface, as supported
558 by the SWI associated peaks (<1cm) or regular peaks of DGT-Cd flux with depth across all of the sites
559 (reference and disposal) and consistent with frequent and regional bloom deposition and burial events.
560 Metals such as Cu and Zn have also been shown to exhibit this behaviour (Lee and Morel, 1995; Wang
561 and Dei, 2001).

562

563 *Linking total metal pool (particulate) and pore-water behaviour:*

564 DGT use also illustrates the lack of agreement between total metal pool determined during routine
565 monitoring of the disposal activity and the metal concentrations/DGT-labile (C_{DGT}) found in pore-
566 waters as highlighted by the DGT flux. There is clear contrast between the total metal particulate
567 reservoir and the release for certain metals. The differences in both DGT profile shape and release of
568 metals in relation to total sediment metal can be seen in Appendix 1, Figure A.1. This is observed in
569 particular for Cd, which is enriched in bulk sediments at the disposal sites but whose source is likely to
570 be linked to phytodetrital decomposition (Fones et al., 2004; Sakellari et al., 2011). Pb and Mn also
571 show enrichment in disposed sediments, but elevated release into the pore-waters is only seen for Mn.

572 For other metals, the DGT data illustrates that release to the pore-waters is controlled by a combination
573 of redox levels (Fe, Mn) and links to Fe/Mn particulate control on partitioning (Pb).

574 Concentrations of metals in the pore-water can also be controlled by other pore-water phases
575 such as the presence of Dissolved Organic Carbon (DOC) or Acid Volatile Sulphides (AVS) (especially
576 Pd, but not Ni) (Lee and Lee, 2005; Duran et al., 2012). It is this control of metal release by and from
577 pore-water particulate compounds (solid phases / colloidal material) and associated within pore-water
578 chemistry that will ultimately control the availability of metal to the resin gel as supplied from the
579 particulate sediment pool (Chifroy et al., 2011). At these sites, free sulphide was below detection limits
580 in the upper parts of the sediment. The controlling behaviour of S^{2-} species on metal pore-water supply
581 is complex and could inhibit/restrict metal release fluxes to a DGT sampler depending on solubility and
582 the prevailing redox or pH conditions (Ankley et al., 1991; Ankley, 1996a; Lee and Lee 2005; Teal et
583 al., 2009; Duran et al., 2012). This control of pore-water chemistry on DGT-metal flux can be seen in
584 the increased release of Pb and Ni to the DGT device at Station C despite no clear relation to drivers
585 such as the total sediment metal pool. This change is also highlighted in the differing behaviour of Ni
586 across all three stations despite an equivalent Ni total sediment pool at all sites.

587 The metal pore-water flux profiles determined in this study illustrate the comparative
588 differences and balance between the metal release from the total particulate pool, pore-water metal
589 chemistry and hence availability to a pore-water sampler such as DGT. The controls on this release are
590 complex and relate to dynamic equilibrium interactions between the total metal particulate pool, the
591 impact of reduction chemistry with depth, and the complexation of released metal ions by pore-water
592 ligands such as sulphur species or organic matter (Chifroy et al., 2011). These chemical interactions
593 within the pore-water will ultimately control metal availability to the DGT and hence metal release
594 within or from the sediment. The understanding of these complex processes is still challenging though
595 the status information provided by the DGT, as a description of labile/bioavailable metal is useful, even
596 without a full understanding of the mechanistic drivers.

597

598 *DGT, bioavailability, bioaccumulation and ecotoxicology:*

599 DGT has often been described as a tool capable of describing the bioavailable fraction of metals in
600 comparison to total metals (Simpson et al., 2007; Simpson et al., 2012; Amato et al., 2015; Ren et al.,
601 2015). This study has illustrated the capacity for DGT to provide vertically resolved metal fluxes to a
602 passive sampler, which could be used as a proxy for a bioavailable fraction. The potential disconnection
603 between total metals and DGT-metal flux observed here has been observed in other studies (see Di
604 Toro 1992; Roulier et al., 2008), although total metals in sediments were the best predictors of
605 bioaccumulation in other studies (Roulier et al., 2008 and references there-in). Some studies have
606 started investigating the links between metal phases (particulate totals, acid extractable, dissolved, DGT
607 fractions) and biological response/load (Simpson et al., 2012). However, further development to
608 demonstrate dose/response from DGT fractions and benthic organisms / effects and appropriate solid

609 phase – pore-water phase modelling would be beneficial. In particular, the complex controls on metal
610 bioavailability created by the interactions within the pore-water chemistry inhibit a mechanistic
611 understanding of the conditions that will promote metal release from a similar total metal pool. The best
612 descriptors of bioavailable metal are still being discussed and evaluated under controlled experimental
613 conditions. An enhanced understanding through combined pore-water metal observational and
614 modelling approaches is needed to enable predictions or risk assessments of metal bioavailability and
615 toxicity to be undertaken in the marine environment under contaminated conditions, including disposal
616 sites.

617 The dynamics between metal supply (particles), metal release and complexation (pore-water)
618 and uptake (bioavailability or bioaccumulation) is a complex one but can be linked to key variables
619 (Dissolved Organic Carbon - DOC, Acid Volatile Sulphide - AVS) in future to further understand
620 release mechanisms and controls. DGT defined fractions may have a role to play here in describing the
621 potential availability and toxicity of a sediment in a similar way to Simultaneously Extractible Metal
622 (SEM) : AVS information (Di Toro et al., 1990; 1992; US EPA , 2005; Simpson et al., 2007; Knox et
623 al., 2012; Simpson et al., 2012). A rapid, depth and space integrated imaging technique such as SPI,
624 which describes iron reduction or sulphide precipitation depths, further aids understanding.

625 The knowledge of the metal release dynamics provided by DGT enhances our ability to describe
626 and explain different biological uptake or impacts observed in sediments of similar total metal
627 concentrations and improves the understanding of the links between total metal, pore-water and
628 biological effects. This description of metal concentration beyond a traditional total measurement is
629 largely missing in local regulatory or regional scale impact or status assessments within the UK or
630 Europe such as OSPAR Quality Status Reports (OSPAR QSR 2010) or ICES reports (ICES WGMS).
631 And yet, improved understanding of the link between hazardous substances and biological responses in
632 sediments is also required as management regulations increasingly require an ecosystem approach. For
633 example, the European Union Marine Strategy Framework Directive (2008/58/EC) includes Descriptor
634 8, which considers the management of sediment contaminant concentrations “*at levels not giving rise*
635 *to pollution effects*” and requires appropriate linkages of benthic system parameters and anthropogenic
636 pressures to invoke a management response (Van Hoey et al., 2010; Borja et al., 2013).

637

638 *Considerations for monitoring applications*

639 A main driver of this study has been to assess the utility of a passive sampler such as DGT to provide
640 better assessment of the risk posed of metal remobilisation from sediments and therefore to aid future
641 sediment activity management. The case study has demonstrated the feasibility by which such relatively
642 cost-effective, easy to use techniques can be built into a monitoring programme alongside the other
643 measures already being sampled. Such a technique can be focused towards site specific contaminant or
644 management (e.g. capping strategies) issues whilst more rapid techniques such as SPI can provide wider
645 spatial context (Germano et al., 2011; Birchenough et al., 2013).

646 In combination with monitoring of total sediment metal, DGT is capable of illustrating areas of metal
647 release, fluxes across the interface and the potential disconnection between total particulate metal pool
648 and pore-water metal. This is especially useful in describing and quantifying a potential pressure or risk
649 associated with metal contamination.

650 Critical within a regulatory framework are also methods to demonstrate and track changes
651 related to an activity, in space/time. This is particularly important for disposal site licensing and
652 monitoring. It is essential to be able to describe changes in metal levels or behaviour in an auditable
653 and defensible way. The comparison of metal profiles between sites has usually occurred by visual
654 comparisons and descriptions, and sometimes regression analysis with depth (Fones et al., 2004).
655 However, this is not statistically robust or makes site comparison difficult, and with higher variances
656 induced by natural sediment heterogeneity or disturbance it is essential to have a method that can detect
657 metal differences within and between sites or changes over time. The statistical modelling of the DGT
658 metal profiles in this study has demonstrated a methodology that allows statistical analysis and
659 investigation of high resolution metal profiles. This approach can provide increased confidence in an
660 assessment of the differences between sites, the site status or processes driving changes in metal levels
661 and distributions and how disposal is affecting them. Despite the high variance, it provides increased
662 ability to determine status/metal flux levels statistically and detect changes over depth, time or space.
663 This is particularly important for detecting changes as a result of a management action or tracking
664 changes after a management action has been implemented. The power of the technique could be
665 improved with increased replication and further investigation of variability with space and time.

666 These insights into metal release (by coupling the DGT measurements and statistical
667 investigation of the profiles) can provide supporting, targeted and complimentary evidence to risk
668 assessments of metal impact at particular locations or for specific questions. The coupling technique is
669 compatible with existing monitoring programmes as documented here. It could be directed towards a
670 specific condition or question highlighted by routine monitoring or total metal assessments. It could
671 also be used to refine total metal trigger levels through improved understanding of the relationship
672 between total metal and pore-water concentrations and resupply (flux). The depth information can also
673 be used to make assessments of metal release risk to the water column under physical disturbances
674 (storms, trawling). Further work would be needed though to give a greater overview of spatial and
675 temporal variability in metal behaviour in relation to total sediment metal levels related to disposal
676 activities and other controlling factors within the sediment matrix, which will dictate metal availability
677 within the pore-water. Combined with rapid spatial techniques such as SPI it might be possible to
678 investigate the disposal site signature and associated changes in metal availability and risk of release
679 under contrasting environmental conditions.

680

681

682 **4.0 Conclusions**

683 The application of high resolution DGT passive samplers to the three sites in this study has improved
684 our understanding of specific metal remobilisation behaviour, contrasting release features between
685 metals, sites and with depth. It has also demonstrated that total particulate metal and DGT-metal flux
686 are not always in agreement, indeed, elevated total particulate metal concentrations do not necessarily
687 lead to high metal release into the sediment pore-waters. This initial application of DGT passive sampler
688 technology, alongside sediment bulk metal analysis, to evaluate metal behaviour at the Souther Point
689 disposal site has highlighted the complex relationship between contaminant disposal load from
690 particulates and metal availability to the pore-water. Furthermore, it has underlined the metal
691 heterogeneity found in the sediments at this disposal site, both between stations and with depth.

692 While bulk sediment analysis for metals gives important information about the quantity of
693 metals present, i.e. the size of the benthic reservoir, and is indicative of the potential hazard, it does not
694 give information about the availability of these metals to the various components of the ecosystem and
695 thus the actual risk posed – either to the benthic community or by flux into the overlying water column
696 and so into the pelagic system. This is where complementary methodology such as DGT enables
697 additional insights. The clear differences in metal flux profiles recorded at different stations, which do
698 not strictly correlate with total metal concentrations in the corresponding slices, illustrate that
699 environmental parameters are influential in regulating fluxes and, by implication, availability of metals.
700 Statistical modelling approaches, as documented here, could be developed in future to describe and
701 track changes in metal behaviour and release across areas and also mechanistically with other metal
702 (metal:metal couples) or environmental controls.

703 In summary, the use of depth resolving passive samples such as DGT is compatible with routine
704 monitoring of disposal sites and can provide valuable additional information. Further work to improve
705 understanding of the controlling factors of metal release to pore-waters, and the likely exposure routes
706 of biota (linked to faunal traits such as feeding modes or sediment location) within the receiving
707 ecosystem as well as corresponding ecotoxicological implications would be beneficial to inform
708 management decisions. Such an increased understanding would not only enable more robust
709 assessments of risks posed by disposal of sediments with high contaminant loads, but could also be used
710 when assessing likely impacts arising from natural events, such as storms, and human activities, such
711 as fishing and changes in controlling parameters under predicted future climate scenarios.

712

713 **Acknowledgements:**

714 This work was supported by Defra and MMO (contract E5403). The views expressed are those of the
715 authors and do not reflect the policies of the funding departments. We gratefully acknowledge the
716 valuable contributions made by the scientific staff and crew of the RV Cefas Endeavour. We also thank

717 Robin Law and three anonymous reviewers for comments to really improve the manuscript and insights
718 our data provided.

719

720 **References:**

721

722 Amato, E.D., Simpson, S.L., Jarolimek, C.V., Jolley, D.F. Diffusive Gradients in Thin Films Technique
723 Provide Robust Prediction of Metal Bioavailability and Toxicity in Estuarine Sediments. *Environ. Sci.*
724 *Technol.*, 2014; 48 (24), 4485–4494.

725

726 Amato, E.D., Simpson, S.L., Belzunce-Segarra, M.J., Jarolimek, C.V., Jolley, D.F. Metal Fluxes from
727 Porewaters and Labile Sediment Phases for Predicting Metal Exposure and Bioaccumulation in Benthic
728 Invertebrates. *Environ. Sci. Technol.*, 2015; 49, 14204–14212.

729

730 Ankley, G.T., Phipps, G.L., Leonard, E.N., Kosian, P.A., Cotter, A.M., Dierkes, J.R. Acid-volatile
731 sulfide as a factor mediating cadmium and nickel bioavailability in contaminated sediments. *Environ*
732 *Toxicol Chem* 1991; 10:1299– 307.

733

734 Ankley, G.T. Evaluation of metal/acid-volatile sulfide relationship in the prediction of metal
735 bioaccumulation by benthic macroinvertebrates. *Environ Toxicol Chem* 1996a; 15:2138– 46.

736

737 Ankley, G.T., Di Toro, D.M., Hansen, D.J., Berry, W.J. Technical basis and proposal for deriving
738 sediment quality criteria for metals. *Environ Toxicol Chem* 1996b; 15:2056– 66.

739

740 Birchenough, A., Bolam, S.G., Bowles, G.M., Hawkins, B. Whomersley, P., Weiss, L. Monitoring of
741 dredged material disposal sites at sea and how it links to licensing decisions. *Proceedings from PIANC*
742 *MMX*, Liverpool, May 2010.

743

744 Birchenough, S.N.R, Boyd, S.E., Coggan, R.A., Limpenny, D.S., Meadows, W.J., Rees, H.L. Lights,
745 camera and acoustics: Assessing macrobenthic communities at a dredged material disposal site off the
746 North East coast of the UK. *Journal of Marine Systems* 2006; 62 (3): 204-216.

747

748 Birchenough, S.N.R., Blake, S.J., Rees, J., Murray, L.A., Mason, C.E., Rees, H.L., Vivian, C.,
749 Limpenny, D.S. Contaminated dredged material: monitoring results from the first capping trial in the
750 U.K. In: 4th International Conference: Proceedings of the Port Development and Coastal Environment.
751 25–28 September 2007, Varna Bulgaria.

752

753 Birchenough, S.N.R., Bolam, S.G., Parker, E.R. SPI-ing on the seafloor: characterising benthic systems
754 with traditional and in situ observations. *Biogeochemistry* 2013; 113 (1-3): 105-11
755

756 Bolam, S.G., Rees, H.L., Somerfield, P., Smith, R., Clarke, K.R., Warwick, R.M., Atkins, M.,
757 Garnacho, E. Ecological consequences of dredged material disposal in the marine environment: a
758 holistic assessment of activities around the England and Wales coastline. *Marine Pollution Bulletin*
759 2010a; 52: 415-426.
760

761 Bolam, S.G., Mason, C., Bolam, T., Whomersley, P., Birchenough, S.N.R, Curtis, M., Birchenough,
762 A., Rumney, H., Barber, J., Rance, J., McIlwaine, P., Law, R.J., Dredged material disposal site
763 monitoring around the coast of England: results of sampling. SLAB5 Project Report, Cefas, UK. 2010b.
764

765 Borja, A., Elliott, M., Marine monitoring during an economic crisis: the cure is worse than the disease.
766 *Mar. Pollut. Bull.* 2013; 68: 1–3.
767

768 Bufflap, S. E., Allen, H. E. Sediment pore water collection methods for trace metal analysis: A review.
769 *Wat. Res.* 1995; 1: 165-177
770

771 Bull, D.C., Williamson, R.B. Prediction of principal metal-binding solid phases in estuarine sediments
772 from colour image analysis. *Environ. Sci.Technol.* 2001; 35:1658-1662.
773

774 Burdige, D.J. *Geochemistry of marine sediments.* Princeton University Press. 2006.
775

776 Butler, E., Leeming, R., Watson, R., Armand, S., Green, M., Final Report on Sediment Resuspension
777 Experiment for Derwent CCI Project. CSIRO Marine Research, Hobart, Tasmania, Australia.
778 <http://www.derwentestuary.org.au/file>. 2005.
779

780 Calmano, W., Hong, J., Forstner, U. Binding and mobilisation of heavy metals in contaminated
781 sediments affected by pH and redox potential. *Water Sci Technol* 1993; 28: 223–35.
782

783 Chapman, P.M., Wang, F., Janssen, C., Persoone, G., Allen, H.E. Ecotoxicology of metals in aquatic
784 sediments: binding and release, bioavailability, risk assessment, and remediation.
785 *Can J Fish Aquat Sci* 1998; 55: 2221–43.
786

787 Ciffroy, P., Nia, Y., Garnier, J.M. Probabilistic Multicompartmental Model for Interpreting DGT
788 Kinetics in Sediments. *Environ Sci Technol* 2011; 45: 9558–9565.
789

790 Dahlqvist, R., Zhang, H., Ingri, J. and Davison, W. Performance of the diffusive gradients in thin films
791 technique for measuring Ca and Mg in freshwater. *Anal Chim Acta* 2002; 460(2): 247-256.
792

793 Davison, W., Zhang, H. In situ speciation measurements of trace components in natural waters using
794 thin-film gels. *Nature* 1994; 367: 546–8.
795

796 Davison, W., Fones, G. R. & Grime, G. W. Dissolved metals in surface sediment and a microbial mat
797 at 100- μ m resolution. *Nature* 1997; 387, 885-888.
798

799 Davison, W., Zhang, H. Progress in understanding the use of diffusive gradients in thin films (DGT) –
800 back to basics. *Environ. Chem.* 2012; 9: 1–13.
801

802 Davison, W., Fones, G.R., Harper, M., Teasdale, P., Zhang, H. Dialysis, DET and DGT: in situ
803 diffusional techniques for studying water, sediments and soils. In: Buffle, J., Horvai, G. (Eds.), *In-Situ*
804 *Monitoring of Aquatic Systems: Chemical Analysis and Speciation*. IUPAC. Wiley, New York, 2000;
805 495–569.
806

807 Davison, W., Zhang, H., Warnken, K.W. Theory and applications of DGT measurements in soils and
808 sediments. In: Greenwood, R., Mills, G., Vrana, B. (Eds.), *Comprehensive Analytical Chemistry*.
809 *Passive Sampling Techniques in Environmental Monitoring*, Elsevier, 2007; 48: 353–378.
810

811 Di Toro, D.M., Mahony, J.D., Hansen, D.J., Scott, K.J., Hicks, M.B., Mayer, S.M., Redmond, M.S.
812 Toxicity of cadmium in sediments: the role of acid volatile sulfide. *Environ Toxicol Chem* 1990;
813 9:1489– 504.
814

815 Di Toro, D.M., Mahony, J.D., Hansen, D.J., Scott, K.J., Carlson, A.R., Ankley, G.T. Acid volatile
816 sulfide predicts the acute toxicity of cadmium and nickel in sediments. *Environ. Sci. Technol.* 1992; 26:
817 96–101.
818

819 Duran, I., Sanchez-Marin, P., Beiras, R. Dependence of Cu, Pb and Zn remobilization on
820 physicochemical properties of marine sediments. *Mar Environ Res* 2012; 77: 43-49.
821

822 Directive 2008/56/EC of the European Parliament and of the Council of 17 June 2008 establishing a
823 framework for community action in the field of marine environmental policy (Marine Strategy
824 Framework Directive).
825

826 Eggleton, J., Thomas, K.V. A review of factors affecting the release and bioavailability of contaminants
827 during sediment disturbance events. *Environ Int* 2004; 30: 973–980.
828

829 Folk, R.L., 1954. The distinction between grain size and mineral composition in sedimentary rock
830 nomenclature. *Journal of Geology* 62 (4), 344-359
831

832 Fones, G.R., Davison, W., Holby, O., Jorgensen, B.B. and Thamdrup, B. High-resolution metal
833 gradients measured by in situ DGT/DET deployment in Black Sea sediments using an autonomous
834 benthic lander. *Limnol Oceanogr* 2001; 46(4): 982-988.
835

836 Fones, G.R, Davison W., Hamilton-Taylor, J. The fine-scale remobilization of metals in the surface
837 sediment of the North-East Atlantic. *Cont Shelf Res* 2004; 24: 1485–1504
838

839 Forstner, U., Wittman, G.T.W. Metal pollution in the aquatic environment. Berlin:
840 Springer-Verlag; 1981.
841

842 Forstner, U., Ahlf, W., Calmano, W., Kersten, M., Salomons, W. Mobility of heavy metals in dredged
843 harbour sediments. In: Sly PG, editor. *Sediments and Water Interactions*.
844 New York: Springer-Verlag. 1986; 371–80.
845

846 Gao, Y., Leermakers, M., Gabelle, C., Divis, P., Billon, G., Ouddane, B., High resolution profiles of
847 trace metals in the pore waters of riverine sediment assessed by DET and DGT. *Sci Total Environ* 2006;
848 362: 266-277.
849

850 Gao, Y., Lesven, L., Gillan, D., Sabbe, K., Billon, G., De Galan, S., Elskens, M., Baeyens, W.,
851 Leermakers, M. Geochemical behaviour of trace elements in sub-tidal marine sediments of the Belgian
852 coast. *Mar Chem* 2009; 117: 88-96.
853

854 Germano JD, Rhoads DC, Valente RM, Carey DA, Solan M. The use of sediment profile imaging (SPI)
855 for environmental impact assessment and monitoring studies: lessons learned from the past four
856 decades. *Oceanogr Mar Biol* 2011; 49:235–298
857

858 Harper, M.P., Davison, W., Zhang, H. and Tych, W. Kinetics of metal exchange between solids and
859 solutions in sediments and soils interpreted from DGT measured fluxes. *Geochim Cosmochim Ac* 1998;
860 62(16): 2757-2770.
861

862 Harper, M.P., Davison, W. and Tych, W. Estimation of pore water concentrations from DGT profiles:
863 A modelling approach. *Aquat Geochem* 1999; 5(4): 337-355.
864

865 ICES Reports from WGMS, accessed on 22nd April 2016, URL:
866 <http://www.ices.dk/community/groups/Pages/WGMS.aspx>
867

868 Knox, A., Paller, M., Roberts, J. Active Capping Technology—New Approaches for *In Situ*
869 Remediation of Contaminated Sediments. *Remediation* 2012; DOI: 10.1002/rem.21313.
870

871 Knox, A. S., Paller, M. H., Milliken, C. E., Redder, T. M., Woolfe, J. R., Seaman, J. Environmental
872 impact of ongoing sources of metal contamination on remediated sediments. *Sci Total Environ* 2016;
873 563-564: 108-117.
874

875 Lee, J., Morel, F.M. Replacement of zinc by cadmium in marine phytoplankton. *Mar Ecol Prog Ser*
876 1995; 127: 305-309.
877

878 Lee, J.-S., Lee, J.-H. Influence of acid volatile sulfides and simultaneously extracted metals on the
879 bioavailability and toxicity of a mixture of sediment-associated Cd, Ni, and Zn to polychaetes *Neanthes*
880 *arenaceodentata*. *Sci Total Environ* 2005; 338: 229– 241
881

882 Lyle, M. The brown-green colour transition in marine sediments: A marker of the Fe(III)–Fe(II) redox
883 boundary, *Limnol. Oceanogr* 1983; 28, 1026–1033.
884

885 Manly, F. J. Randomization, Bootstrap and Monte Carlo Methods in Biology: 2nd edition. Chapman and
886 Hall, London. 2008
887

888 Mason, C. NMBAQC's Best Practice Guidance. Particle Size Analysis (PSA) for Supporting Biological
889 Analysis. National Marine Biological AQC Coordinating Committee, 72pp, Dec. 2011.
890

891 Merritt, K.A., Amirbahman, A. Mercury dynamics in sulfide-rich sediments: Geochemical influence on
892 contaminant mobilization within the Penobscot River estuary, Maine, USA *Geochim Cosmochim Acta*.
893 2007; 71: 929–941.
894

895 MEMG Group Co-ordinating Sea Disposal Monitoring. Final Report of the Dredging and Dredged
896 Material Disposal Monitoring Task Team. Science Series Aquatic Environmental Monitoring Reports,
897 CEFAS, Lowestoft, (55): 52pp. 2003
898

899 Oporto, C., Smolders, E., Degryse, F., Verheyen, L. and Vandecasteele, C. DGT-measured fluxes
900 explain the chloride-enhanced cadmium uptake by plants at low but not at high Cd supply. *Plant Soil*
901 2009; 318(1-2): 127-135.

902

903 OSPAR. Quality Status Report (QSR) 2010. OSPAR Commission, London, 2010: 176 pp.

904

905 Panther, J.G., Bennett, W.W., Welsh, D.T. and Teasdale, P.R. Simultaneous Measurement of Trace
906 Metal and Oxyanion Concentrations in Water using Diffusive Gradients in Thin Films with a Chelex-
907 Metsorb Mixed Binding Layer. *Anal Chem* 2014; 86(1): 427-434.

908

909 Peijnenburg, W. J. G. M., Teasdale, P. R., Reible, D., Mondon, J., Bennett, W. W., Campbell, P. G. C.
910 Passive sampling methods for contaminated sediments: State of the science for metals. *Integrated*
911 *Environmental Assessment and Management*. 2014; 10(2): 179–196.

912

913 R Development Core Team. R: a language and environment for statistical computing. R Foundation
914 for Statistical Computing, Vienna, Austria. ISBN 3-900051-07-0, <http://www.R-project.org>. 2010

915

916 Rabouille, C., Denis, L., Dedieu, K., Stora, G., Lansard, B., Grenz, C. Oxygen demand in coastal marine
917 sediments: comparing in situ microelectrodes and laboratory core incubations *J Exper Mar Biol Ecol*
918 2001; 285/286: 49–69.

919

920 Rees, H.L., Pendle, M.A., Limpenny, D.S., Mason, C.E., Boyd, S.E., Birchenough, S., Vivian,
921 C.M.G. Benthic responses to sewage-sludge disposal and climate events in the Western North Sea. *J.*
922 *Mar. Biol. Assoc. UK*. 2006; 86: 1–18.

923

924 Ren, J., Williams, P.N., Luo, J., Ma, H., Wang, X. Sediment metal bioavailability in Lake Taihu, China:
925 evaluation of sequential extraction, DGT, and PBET techniques. *Environmental Science and Pollution*
926 *Research*. 2015; 22 (17), 12919-12928.

927

928 Rhoads, D.C., Germano, J.D. Characterization of organism-sediment relations using sediment profile
929 imaging: an efficient method of remote ecological monitoring of the seafloor. *Mar Ecol Prog Ser* 1982;
930 8:115-128

931

932 Roulier, J.L., Tusseau-Vuillemin, M.H., Coquery, M., Geffard, O., Garric, J. Measurement of dynamic
933 mobilization of trace metals in sediments using DGT and comparison with bioaccumulation in
934 *Chironomus riparius*: First results of an experimental study. *Chemosphere* 2008; 70: 925–932.

935

936 Rowlatt, S.M., Rees, H.L., Limpenny, D.S. & Allen, J. Sediment quality of the north-east coast of
937 England. International Council for the Exploration of the Sea (CM Papers and
938 Reports) 1989; CM1989/E:16, 21pp.
939

940 Rowlatt, S.M., Ridgeway, I.M. Final reports of the metals task team and the organics task team. Science
941 Series, Aquatic Environment Monitoring Report, Cefas, Lowesoft, 1997; No. 49,
942 51 pp.
943

944 Sakellari, A., Plavsi, M., Karavoltzos, S., Dassenakis, M., Scoullou, M. Assessment of copper,
945 cadmium and zinc remobilization in Mediterranean marine coastal sediments. *Estuar Coast Shelf Sci*
946 2011; 91: 1-12.
947

948 Sapp, M., Parker, E.R., Teal, L.R., Schratzberger, M. Advancing the understanding of biogeography-
949 diversity relationships of benthic microorganisms in the North Sea. *FEMS Microbiol Ecol* 2010; 74:
950 410-429.
951

952 Scally, S., Davison, W., Zhang, H. Diffusion coefficients of metals and metal complexes in hydrogels
953 used in diffusive gradients in thin films, *Anal. Chim. Acta* 2006; 558: 222-229.
954

955 Schintu, M., Marras, B., Durante, L., Meloni, P. and Contu, A. Macroalgae and DGT as indicators of
956 available trace metals in marine coastal waters near a lead-zinc smelter. *Environ Monit Assess* 2010;
957 167(1-4): 653-661.
958

959 Shiva, A.H., Teasdale, P.R., Bennett, W.W. and Welsh, D.T. A systematic determination of diffusion
960 coefficients of trace elements in open and restricted diffusive layers used by the diffusive gradients in
961 a thin film technique. *Anal Chim Acta* 2015; 888: 146-154.
962

963 Shiva, A.H., Bennett, W.W., Welsh, D.T. and Teasdale, P.R., 2016. In situ evaluation of DGT
964 techniques for measurement of trace metals in estuarine waters: a comparison of four binding layers
965 with open and restricted diffusive layers. *Environ Sci Proc Imp* 2016; 18(1): 51-63.
966

967 Simpson, S. L., Batley, G. E. Predicting metal toxicity in sediments: A critique of current approaches.
968 *Integr. Environ. Assess. Manage.* 2007; 3, 18–31.
969

970 Simpson, S. L., Yverneau, H., Cremazy, A., Jarolimek, C. V., Price, H., Jolley, D. F. DGT-induced
971 copper flux predicts bioaccumulation and toxicity to bivalves in sediments with varying properties.
972 *Environm Sci Technol* 2012; 46 (16): 9038-9046.

973 Stockdale, A., Davison, W., Hao, Z. Micro-scale biogeochemical heterogeneity in sediments: A review
974 of available technology and observed evidence. *Earth-Sci Rev* 2009; 92: 81-97.
975

976 Tankere-Muller, S., Zhang, H. Fine scale remobilisation of Fe, Mn, Co, Ni, Cu and Cd in contaminated
977 marine sediment. *Mar Chem* 2007; 106 (1-2): 192-207.
978

979 Teal, L. R., Parker, R., Fones, G., Solan, S. Simultaneous determination of in situ vertical transitions of
980 color, pore-water metals, and visualisation of infaunal activity in marine sediments. *Limnol Oceanol*
981 2009; 54 (5): 1801-1810.

982 Teal, L.R., Parker, E.R., Solan, M. Sediment mixed layer as a proxy for benthic ecosystem process and
983 function *Mar. Ecol. Prog. Ser* 2010; 298: 79–94.
984

985 Teal, L.R., Parker, E.R.; Solan, M. Coupling bioturbation activity to metal (Fe and Mn) profiles in situ.
986 *Biogeosciences* 2013; 10: 2365 – 2378.
987

988 Teasdale, P.R., Hayward, S., Davison, W. In situ, high-resolution measurement of dissolved sulfide
989 using diffusive gradients in thin films with computer-imaging densitometry. *Anal Chem* 1999; 71:
990 2186–2191.
991

992 Turner, G. S. C., Mills, G. A., Teasdale, P. R., Burnett, J. L., Amos, S. & Fones, G. R. Evaluation of
993 DGT techniques for measuring inorganic uranium species in natural waters: Interferences, deployment
994 time and speciation. *Anal Chim Acta* 2012; 739: 37-46.
995

996 Turner, G. S. C., Mills, G. A., Bowes, M. J., Burnett, J. L., Amos, S. & Fones, G. R. Evaluation of DGT
997 as a long-term water quality monitoring tool in natural waters; uranium as a case study. *Environ Sci*
998 *Proc Imp* 2014; 16(3): 393-403.
999

1000 U.S. EPA. Procedures for the Derivation of Equilibrium Partitioning Sediment Benchmarks
1001 (ESBs) for the Protection of Benthic Organisms: Metal Mixtures (Cadmium, Copper, Lead,
1002 Nickel, Silver and Zinc). EPA-600-R-02-011. Office of Research and Development. Washington,
1003 DC 20460 2005.
1004

1005 Van Hoey, G., Borja, A., Birchenough, S., Buhl-Mortensen, L., Degraer, S., Fleischer, D., Kerckhof,
1006 F., Magni, P., Muxika, I., Reiss, H., Schroder, A. & Zettler, M. L. The use of benthic indicators in
1007 Europe: From the Water Framework Directive to the Marine Strategy Framework Directive. *Mar Poll*
1008 *Bull* 2010; 60, 2187-2196.

1009 Verardo, D.J., Froelich, P.N., McIntyre, A. Determination of organic carbon and nitrogen in marine
1010 sediments using the Carlo Erba NA-1500 analyzer. *Deep-Sea Res* 1990; 37: 157–165.
1011

1012 Wang, W.-X., Dei, R.C. Metal uptake in a coastal diatom influenced by major nutrients (N, P and Si)
1013 *Wat Res* 2001; 35 (1): 315-321.
1014

1015 Wood, S.N. *Generalized Additive Models: An Introduction with R*. Chapman and Hall/CRC, London.
1016 2006.
1017

1018 Zhang, H., Davison, W., Miller, S. and Tych, W. In-situ high-resolution measurements of fluxes of Ni,
1019 Cu, Fe, and Mn and concentrations of Zn and Cd in porewaters by DGT. *Geochim Cosmochim Ac*
1020 1995; 59(20): 4181-4192.
1021

1022 Zhang, H. and Davison, W. Diffusional characteristics of hydrogels used in DGT and DET techniques.
1023 *Anal Chim Ac* 1999; 398(2-3): 329-340.
1024

1025 Zhang, H. and Davison, W. Direct in situ measurements of labile inorganic and organically bound metal
1026 species in synthetic solutions and natural waters using diffusive gradients in thin films. *Anal Chem*
1027 2000; 72(18): 4447-4457.
1028
1029